

Mesoscale fluxes over heterogeneous flat landscapes for use in larger scale models

Roger A. Pielke*, Xubin Zeng, Tsengdar J. Lee, Giovanni A. Dalu

Department of Atmospheric Science, Colorado State University, Fort Collins, CO 80523, USA

Abstract

We have developed a framework to parameterize mesoscale fluxes of heat, moisture, and momentum, in a cloud-free environment, which result from heterogeneous heating of flat land surfaces. The importance and parameterizability of these mesoscale fluxes is demonstrated using the mathematical concept of predictability. This methodology is used to estimate the relative importance of mesoscale, as contrasted with turbulent fluxes, in the Konza Prairie of Kansas during the FIFE field experiment. © 1997 Elsevier Science B.V.

1. Introduction

During the last decade or so, procedures to represent landscape heterogeneity within a larger scale area, such as a general circulation model (GCM) grid cell, have focused on a summation of surface fluxes within that area, proportionally weighted by the fluxes from each land surface type. Examples of this approach are reported by a number of authors (Avisar and Pielke, 1989; Kosta and Suarez, 1992; Bonan et al., 1993; Henderson-Sellers et al., 1993; Miller, 1993; Arritt and Clark, 1994; Li and Avisar, 1994).

There is convincing modeling evidence, however, that mesoscale¹ fluxes that result from landscape heterogeneity in flat terrain can often be as large as and larger than

* Corresponding author.

¹We define mesoscale using the definition presented in Pielke (Pielke, 1984). Mesoscale systems can be accurately described by the hydrostatic equations of motion, while the turbulent motions are non-hydrostatic features. Mesoscale features differ from larger scale systems in that the horizontal winds are substantially out of gradient wind balance even above the planetary boundary layer.

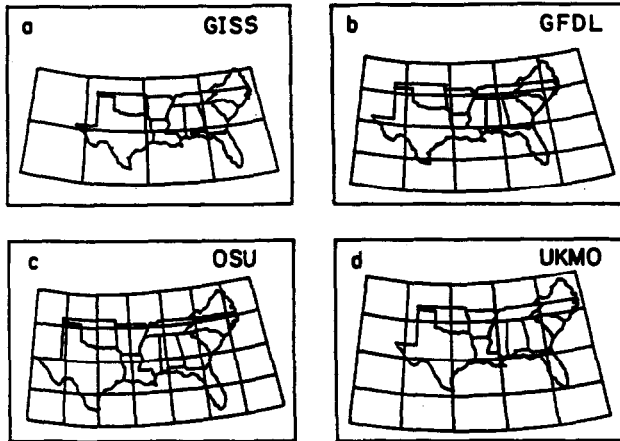


Fig. 1. Horizontal resolution of four GCMs across the southern US: (a) GISS, (b) GFDL, (c) OSU, and (d) UKMO (from Cooter et al., 1993).

turbulent fluxes, as well as have a different vertical distribution than the turbulent fluxes averaged over the scale of a GCM grid such as illustrated in Fig. 1. Examples of studies that document the modification of atmospheric boundary layer structure, and/or the development of mesoscale flow owing to land surface inhomogeneity are reported by a number of authors (Avisar and Pielke, 1989; André et al., 1989a; Raupach, 1991; Dalu et al., 1991a,b; Pielke et al., 1991, 1993a; Cotton and Pielke, 1995; Segal and Arritt, 1992; Manqian and Jinjun, 1993; Avisar and Chen, 1993; Guo and Schuepp, 1994). A number of these papers are summarized in Cotton and Pielke (Cotton and Pielke, 1995). These mesoscale fluxes have substantial coherent structure such that they are predictable features (i.e. Zeng, 1992; Zeng and Pielke, 1993a). Observations have documented the importance of heterogeneous landscape in influencing boundary layer structures and mesoscale fluxes (Balling, 1988; Segal et al., 1988, 1989; Beljaars and Holtslag, 1991; Doran et al., 1992; Smith et al., 1992; Mahrt and Ek, 1993; Mahrt et al., 1994a,b) and in effecting such related properties as soil water infiltration (Wood et al., 1992).

Therefore, it should be possible to parameterize the influence of the mesoscale fluxes on larger scale atmospheric structures. This is the purpose of this paper. Claussen (Claussen, 1991), for example, has discussed how land surface variability influences spatially averaged fluxes and spatially averaged vertical gradients, although his analysis is limited to the situation where the boundary layer becomes homogeneous above a 'blending height' (Wierenga, 1986), which is situated within the surface layer. Mahrt (Mahrt, 1987) and Mason (Mason, 1988) also have papers that are concerned with this topic. Lynn and coworkers (Lynn et al., 1995) are also developing a new procedure to parameterize mesoscale fluxes resulting from landscape patches.

Field programs which focus on land surface-atmosphere interactions such as FIFE (Sellers et al., 1992a; Betts and Beljaars, 1993) in Kansas, USA; BOREAS (see Sellers et al., 1995) in Saskatchewan and Manitoba, Canada; LOTREX (Schädler et al., 1990) in Hildesheimer Börde, Germany; EFEDA (Bolle et al., 1993) in Spain; HAPEX-MOBILHY

(André et al., 1989b; Noilhan et al., 1991) in France; HAPEX-NIGER92 (e.g. Gash et al., 1991); SEBEX (Wallace et al., 1991) in the Sahel of Africa and in the Amazon region (e.g. Shuttleworth, 1985; Wright et al., 1992; Gash and Shuttleworth, 1991) can provide an observational data base to contrast with the model results.

2. Methodology

Linear studies can provide us with some insight as to when mesoscale circulations are likely to generate vertical fluxes of heat, moisture, and momentum on the same order as turbulent fluxes. Dalu and Pielke (Dalu and Pielke, 1993) report on one such modeling effort where linear response of the atmosphere to heat patches of various sizes in flat terrain are examined. Based on that analysis and for the case of zero large-scale flow, horizontal fluxes can homogenize the atmosphere a short distance above the surface (such that horizontal gradients in boundary layer structure do not develop) when

$$K_x \left(\frac{m\pi}{R_0} \right)^2 T F_1(t_m) = \text{Order } (1) \quad (1)$$

where R_0 is the Rossby radius of deformation, T is proportional to the inertial period and a period related to deceleration of horizontal flow, $m = 2R_0/L_x$, and $F_1(t_m)$ is the time-dependent evolution of the mesoscale circulation. K_x is the horizontal exchange coefficient. L_x is the horizontal spatial scale of the heat patches. Claussen (Claussen, 1991) defines the height at which the atmosphere homogenizes (i.e. the blending height) as the level with the same scale as the vertical diffusion length scale.

The product of variables in Eq. (1) is of order unity, as discussed in Dalu and Pielke (Dalu and Pielke, 1993), when

$$m = \frac{1}{\pi} \left[\frac{N_0 h_0 R_0}{F_1(t_m) K_x} \right]^{\frac{1}{2}}$$

where $N_0 = [(g/\theta)\partial\theta/\partial z]^{\frac{1}{2}}$ (i.e. the Brunt–Väisälä frequency) and h_0 is the maximum depth of the planetary boundary layer. Using these relations, at high wavenumbers (i.e. large m), for example, with $m = 100$ ($L_x = 2$ km), the mesoscale fluxes from this patch size would be important all day for $K_x = 10 \text{ m}^2 \text{ s}^{-1}$ (for this example, $R_0 = 100$ km, $h_0 = 1.5$ km, $T = 10^4$ s, and $N_0 = 10^{-2} \text{ s}^{-1}$ were defined). If $K_x = 100 \text{ m}^2 \text{ s}^{-1}$, however, only patches having a wavenumber less than or equal to 30 ($L_x = 7$ km) would produce significant mesoscale fluxes throughout the day. With this large value of K_x , the $L_x = 2$ km patches would have significant fluxes relative to the turbulent fluxes only for a very short time in the morning, if the diurnal heating of the patches was the dominant surface forcing mechanism. This analytic model indicates that mesoscale fluxes (and thus, the need to parameterize them) become insignificant when the horizontal scale of the flow is on the same order as the vertical scale (i.e. $R_0/m \cong h_0$). Avissar and Pielke (Avissar and Pielke, 1989) assumed this

result, but without theoretical justification, in developing a mosaic one-dimensional representation of land surface effects.

Using mixed-layer scaling (e.g. see Garratt, 1992), the horizontal exchange coefficient can be estimated as

$$K_x \cong l\sigma_H$$

where for a mixed layer $\sigma_H = u_* (12 + 0.5h_0/|L|)^{1/3}$ and $l = 1.5h_0$ (e.g. see Pielke, 1984, pp. 177–178) can be used. The parameter u_* is the friction velocity and L is the Monin length. From this analysis, as the heat patches become smaller, their influence is more easily mixed horizontally, as a function of height above the surface (as an example, with $u_* = 0.5 \text{ m s}^{-1}$, $h_0 = 1.5 \text{ km}$, $|L_x| = 10 \text{ m}$, yields $K_x = 8.55 \times 10^3 \text{ m}^2 \text{ s}^{-1}$). This intensity of horizontal mixing also depends on the thermodynamic stability in the lower atmosphere, in which more vigorous convective heating would result in stronger horizontal mixing.

The introduction of large-scale wind flow modifies the importance of mesoscale fluxes, as shown by Pielke and coworkers (Pielke et al., 1993b), with stronger mesoscale fluxes where the large-scale flow is opposite in direction and about the same magnitude of speed as the resultant mesoscale induced horizontal wind flow. Otherwise, the presence of a large-scale wind reduces the importance of mesoscale fluxes for the same size surface heat patch scale. This large-scale wind dilutes the influence of the heat patches when they are sufficiently small by advecting warm air over colder surfaces, and colder air over the warmer patches, thereby promoting homogenization above the surface as a result of this advection and destabilization of the atmosphere over the warmer surfaces. This effect was demonstrated in a set of large eddy model simulations over flat terrain reported by Hadfield and coworkers (Hadfield et al., 1991, 1992).

To determine whether we can parameterize mesoscale and turbulent fluxes associated with landscape patchiness, we first have explored the predictability of these flows. The predictability measure that we apply is the signal-over-noise ratio, r . The signal is defined to be the domain-averaged root mean square (rms) difference of a variable at time t and at the initial time, and the noise is defined to be domain-averaged rms difference of a variable in the control simulation and in the perturbed simulation at time t . The domain average is obtained from a vertical and horizontal summation of each grid point in the domain. In order to estimate the overall predictability during the day, we have also computed the mean value \bar{r} , of the signal-over-noise ratio $r(t)$ from $t = 3$ to 11 h. When $\bar{r}(a) \geq 1$ the variable a is defined to be predictable during the day, otherwise the variable a is unpredictable. Fig. 2, Fig. 3 and Fig. 4 show \bar{r} of θ , u , and w as a function of the synoptic wind U and the patch size L_x , respectively. It is seen that $\bar{r}(\theta)$ is always larger than unity. For most of the parameter space, $\bar{r}(\theta)$ is about 10. $\bar{r}(u)$ is greater than unity except when both U and L_x are small. For most of the parameter space, $\bar{r}(w)$ is greater than unity.

In Fig. 2, Fig. 3 and Fig. 4, when L_x is small, \bar{r} is relatively small because surface differential heating is small. In Fig. 3 and Fig. 4 (for u and w), as L_x increases, \bar{r} decreases. The reason is that when L_x is large, except near the coastal area, the domain is dominated by boundary layer turbulence, just like the homogeneous case. This has

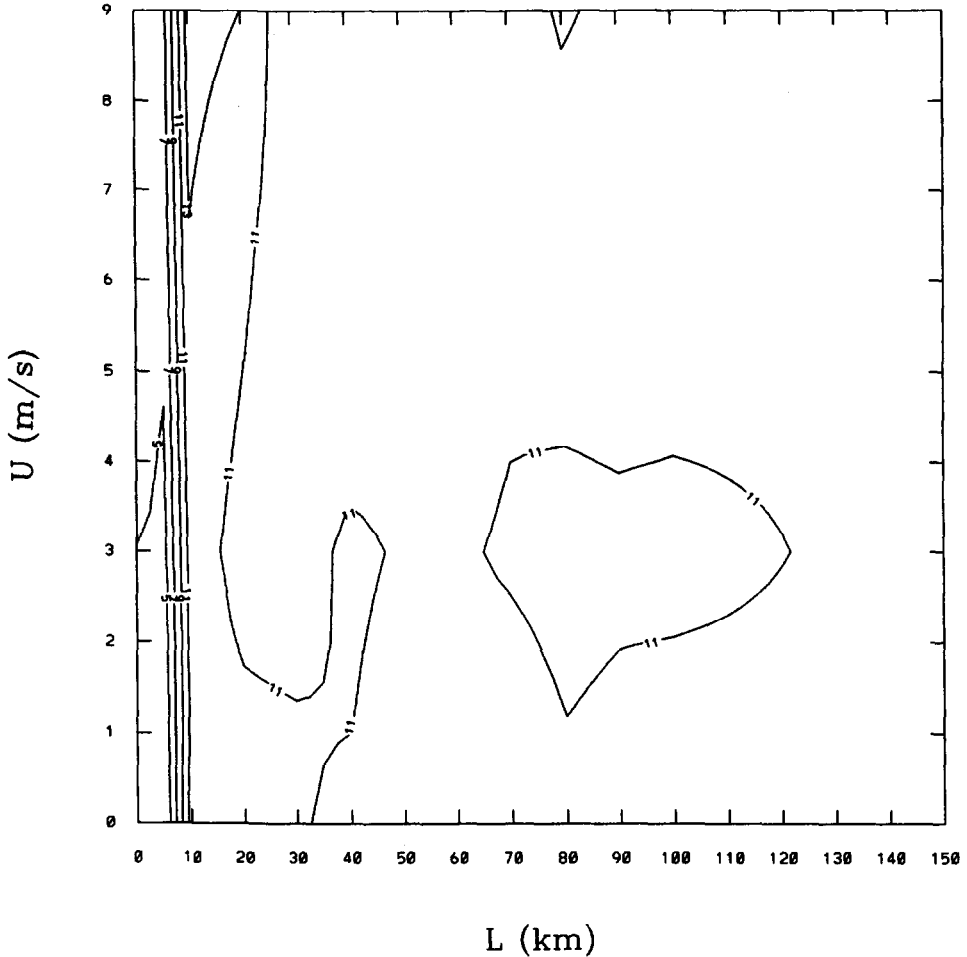


Fig. 2. The temporal- and domain-averaged signal-over-noise ratio of θ as a function of the synoptic wind U and the patch size L . The isolines are drawn with values of 5, 7, 9, and 11. The maximum value is 13.8 and the minimum value is 3.45.

been discussed in Zeng and Pielke (Zeng and Pielke, 1993a). Further discussions on the predictability of surface-induced flow are given elsewhere (Zeng and Pielke, 1993b, 1995a).

Since there exists predictability for a wide range of values of synoptic wind flow and patch size, this indicates that we should be able to develop a parameterization of mesoscale and turbulent fluxes over this parameter space.

Analogous to mixed-layer boundary layer scaling and similarity scaling, we hypothesize that there exist non-dimensional scaling parameters that can be used to evaluate the importance of mesoscale fluxes over heterogeneous, flat terrain.

The assumed non-dimensional parameters to be functionally related to the mesoscale

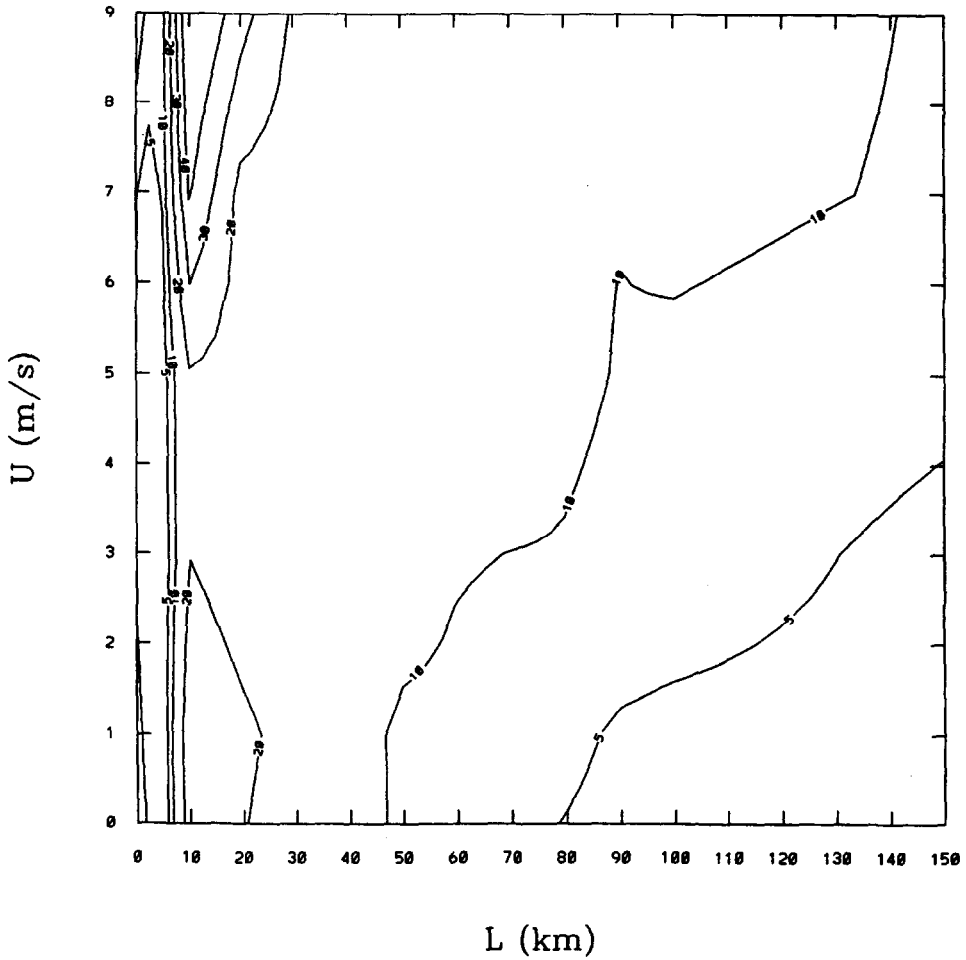


Fig. 3. The temporal- and domain-averaged signal-over-noise ratio of u as a function of the synoptic wind U and the patch size L_x . The isolines are drawn with values of 1, 5, 10, 20, 30, and 40. The maximum value is 52.6 and the minimum value is 0.68.

fluxes are

$$R_b = (gz_i \delta \theta) / (\theta_s U^2)$$

$$z_i / L_x$$

$$\lambda_1 = U z_i / L_x w_*$$

$$\lambda_2 = U^2 / c_p \Delta \theta$$

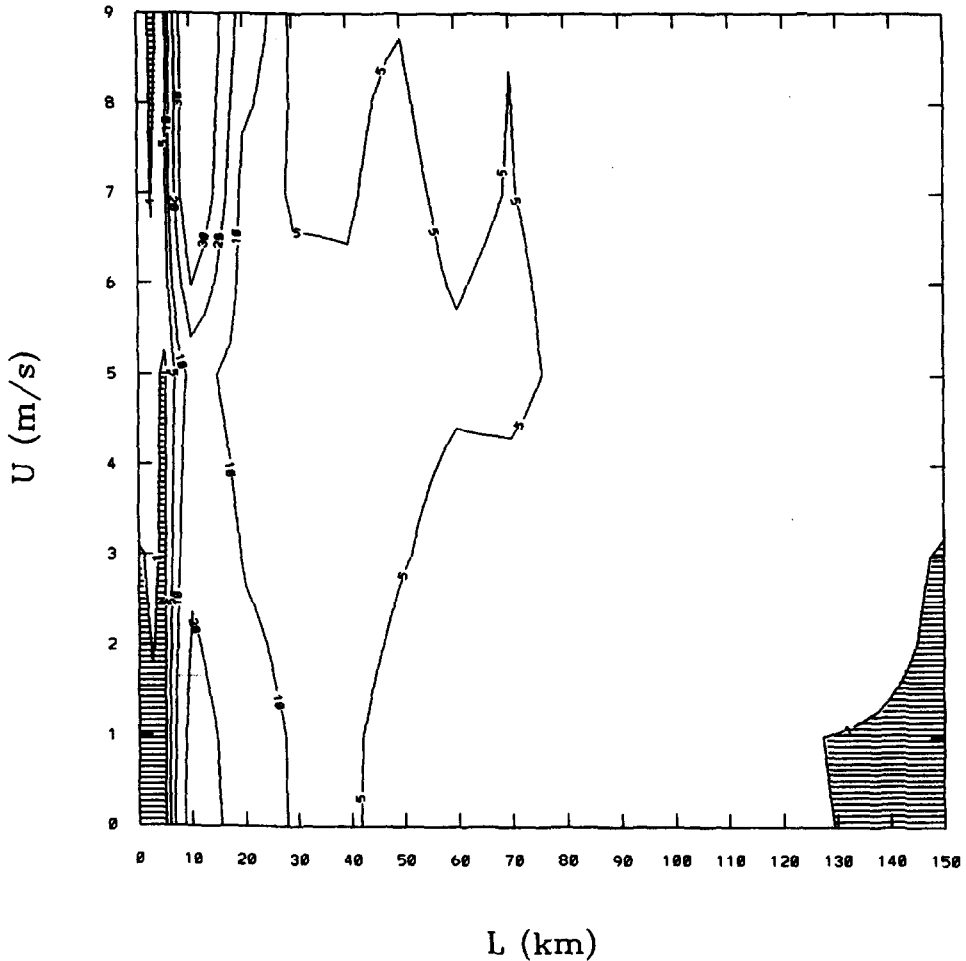


Fig. 4. The temporal- and domain-averaged signal-over-noise ratio of w as a function of the synoptic wind U and the patch size L_x . The isolines are drawn with values of 1, 5, 10, 20, and 30. The maximum value is 49.2 and the minimum value is 0.45.

U is the large-scale advection wind estimated as the synoptic flow at the boundary layer height z_i , while $\Delta\theta$ is the maximum horizontal surface temperature difference at the roughness height z_0 , between different patches. L_x is the dominant horizontal patch size and $\delta\theta$ is the potential temperature difference between the depth z_i , and the surface. The potential temperature at z_0 is θ_s , and $w_* = (gQ_s z_i / \theta_s)^{1/3}$ where Q_s is the turbulent surface sensible heat flux. The parameter, w_* , is the convective velocity scale. Each of these parameters can be estimated from the resolvable variables in larger scale models, except $\Delta\theta$ and L_x . These two parameters, however, could be obtained using a mosaic approach (e.g. Avissar and Pielke, 1989; Avissar and Verstraete, 1990; Miller, 1993) where

vegetation, soil, and water coverage information are used to obtain such information as leaf area index, soil moisture, etc. within subareas of a larger scale model grid cell. R_b provides a measure of the intensity of convective turbulent generation while z_i/L_x is a measure of the depth, z_i , into the atmosphere in which this turbulence would extend relative to the dominant horizontal patch size, L_x . Horizontal gradients in turbulent sensible heating, and the depth, z_i , to which this heating extends are what generates mesoscale circulations. λ_1 yields a measure of the relative importance of horizontal advection to convective vertical mixing, while λ_2 is a ratio related to horizontal advection and the horizontal pressure gradient force, as introduced in Pielke (Pielke, 1984, Chapter 3).

Besides these four independent parameters, we have also suggested another four

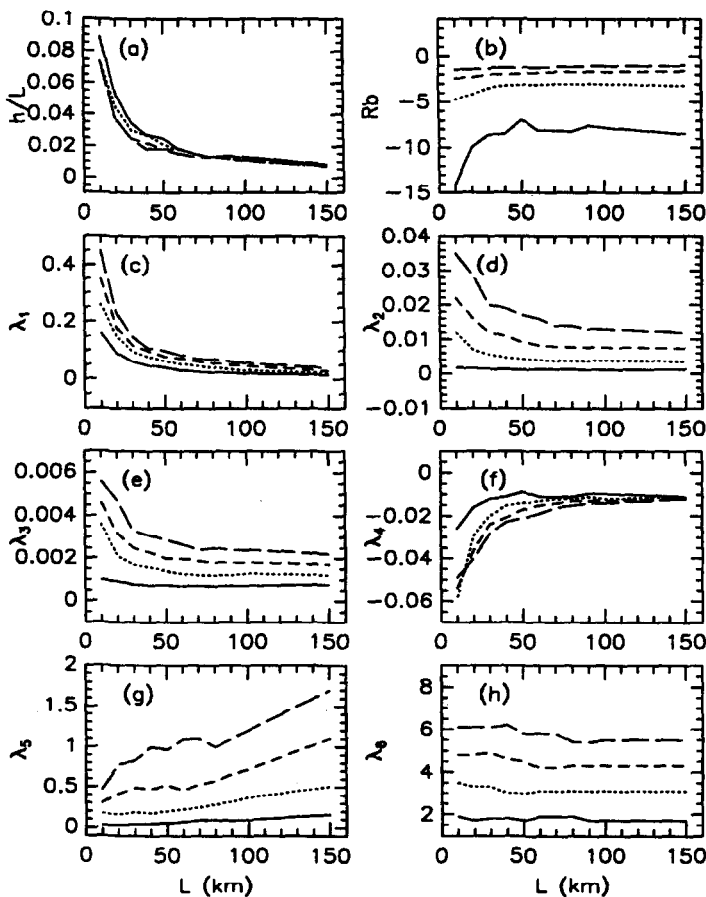


Fig. 5. The eight dimensionless parameters as a function of the horizontal scale L_x of the surface heat patches and the synoptic wind U at time $t=8$ h after sunrise. The cases with $U=3, 5, 7, 9$ m s⁻¹ are represented by the solid, dotted, short-dashed, and long-dashed lines, respectively.

parameters and they are

$$\lambda_3 = \lambda_2 z_i / (\lambda_1 L_x) = U w_* / (c_p \Delta \theta)$$

$$\lambda_4 = \lambda_2 R_b = g z_i \delta \theta / (\theta_s c_p \Delta \theta)$$

$$\lambda_5 = \lambda_2 L_x / z_i = L_x U^2 / (z_i c_p \Delta \theta)$$

$$\lambda_6 = \lambda_1 L_x / z_i = U / w_*$$

We expect that mesoscale fluxes would vary in a non-linear fashion when these parameters vary, but would be a well-defined function of these effects. For example, mesoscale effects would be expected to dominate for intermediate values of L_x (Xian and Pielke, 1991; Avissar and Chen, 1993). For very small values of L_x , the atmosphere is quickly homogenized immediately above the surface such that mesoscale circulations do not develop (e.g. Hadfield et al., 1991, 1992). For very large values of L_x , mesoscale circulations would develop only near the patch edge with the interiors dominated by turbulent fluxes. This paper places quantitative limits on the influence of these parameters on the flux.

In order to explore the parameter space of the above parameters, in order to assess the value of this parameterization approach, and to study the relationship between mesoscale, turbulent, and total fluxes, we have performed extensive two-dimensional numerical models by means of the Colorado State University-Regional Atmospheric Modeling System (CSU-RAMS; Pielke et al., 1992). The non-hydrostatic equations are used with moisture taken as a passive tracer. Radiation, subgrid-scale turbulence, and soil model parameterizations are included. The horizontal grid intervals are $\Delta x = 2$ km, and periodic lateral boundary conditions are used. A more detailed model description has been given in Zeng and Pielke (Zeng and Pielke, 1993a). The surface consists of alternate strips of water and land with strip sizes of $L = 10, 20, \dots, 100, \text{ and } 150$ km. The synoptic wind is $U = 3, 5, 7, \text{ and } 9$ m s⁻¹. When U is smaller than 3 m s⁻¹, some of the above parameters are either too small or too large, and the above parameters need to be modified; e.g. replacing U by $(U + w_*)$. This issue will be addressed in future work.

Fig. 5 illustrates how the values of the eight parameters vary as a function of the horizontal scale (L) of surface heat patches and the synoptic wind U . Relatively smooth curves are observed in Fig. 5, which is a necessary condition in order to properly parameterize different fluxes as a function of these parameters. Fig. 5 also represents the part of the parameter space that we have explored.

3. Parametrization form

While there still needs to be additional model runs to explore the entire spectrum of meteorological conditions, there is sufficient robustness to the model runs to present the

Table 1

The parameters P_i used in eqn (2) for mesoscale (denoted by superscript "'") and small-scale (or turbulent) (denoted by superscript "'") sensible heat, moisture, and momentum fluxes scaled by their corresponding total (turbulent) surface values

Dimensionless fluxes	P_1	P_2	P_3
Mesoscale flux			
$\langle w'\theta' \rangle$	λ_4	λ_6	z/L_x
$\langle w'q' \rangle$	λ_2	λ_4	λ_6
$\langle w'u' \rangle$	λ_1	z/L_x	R_b
Turbulent flux			
$\langle w''\theta'' \rangle$	λ_4	z/L_x	R_b
$\langle w''q'' \rangle$	λ_1	λ_3	z/L_x
$\langle w''u'' \rangle$	λ_4	z/L_x	R_b

functional form of the algorithm for the large-scale averaged mesoscale, turbulent, and total fluxes.

These fluxes are strongly dependent upon the dimensionless height z/z_i . Schematically, our parameterization equation for any dimensionless flux F can be written as

$$F - f_1(z/z_i) = g\left(\frac{z_i}{L}, R_b, \lambda_1, \dots, \lambda_6\right) f_2(z/z_i) \quad (2)$$

In our study, the function f_1 is a quadratic or cubic polynomial and the function f_2 is a linear or quadratic polynomial (or this polynomial multiplied by $f_1(z/z_i)$). The function g is a linear or quadratic polynomial of each parameter.

There are two conflicting requirements on a parameterization scheme: the scheme should use a functional form as simple as possible, and should use as few parameters as possible; and the scheme should be as accurate as possible. To balance these two requirements, we propose the following parameterization equations for domain-averaged (i.e. large-scale model grid-box-averaged), mesoscale (with the superscript "'"), turbulent (with the superscript "'"), and total fluxes of sensible heat $\langle w\theta \rangle$, latent heat $\langle wq \rangle$, and momentum $\langle wv \rangle$ in the boundary layer. These equations have been tested against model-generated data at time $t = 7, 7.5, \text{ and } 8$ h after sunrise based on statistical techniques which are discussed in Zeng and Pielke (Zeng and Pielke, 1995b).

For mesoscale fluxes, which are defined in this paper as the resolvable flux with respect to model grids with $\Delta_x = 2$ km, and small-scale (or turbulent) fluxes, which are defined as the subgrid parameterized fluxes in this model grid, the general formula is

$$\frac{F - f_1\left(\frac{z}{z_i}\right)}{f_1\left(\frac{z}{z_i}\right)} = (a_1 + a_2 p_1 + a_3 p_1^2 + a_4 p_2 + a_5 p_2^2 + a_6 p_3 + a_7 p_3^2) + (b_1 + b_2 p_1 + b_3 p_1^2 + b_4 p_2 + b_5 p_2^2 + b_6 p_3 + b_7 p_3^2) \frac{z}{z_i} \quad (3)$$

where F is a flux scaled by its total (or turbulent) surface value, p_i ($i = 1, 2, \text{ and } 3$) represent

Table 2

The coefficients a_i used in Eq. (2) for mesoscale (denoted by superscript 'm') and small-scale (or turbulent) (denoted by superscript 't') sensible heat, moisture, and momentum fluxes scaled by their corresponding total (or turbulent) surface values

Dimensionless fluxes	a_1	a_2	a_3	a_4	a_5	a_6	a_7
Mesoscale flux							
$\langle w'\theta' \rangle$	2.57	249.20	2735.80	-0.202	0.209×10^{-1}	88.65	-687.20
$\langle w'q' \rangle$	7.35	597.70	-8507.40	322.70	3620.00	-2.20	0.889×10^{-1}
$\langle w'u' \rangle$	0.305	-80.64	137.10	461.10	-4762.10	0.724	0.751×10^{-1}
Turbulent flux							
$\langle w'\theta^t \rangle$	-0.908×10^{-2}	-4.01	-77.50	-2.32	23.30	0.597×10^{-2}	-0.139×10^{-3}
$\langle w'q^t \rangle$	-0.523	-5.01	8.77	430.70	-73761.80	20.20	-133.10
$\langle w'u^t \rangle$	0.272×10^{-2}	16.90	169.60	11.50	-119.90	-0.365×10^{-2}	0.349×10^{-3}

Table 3

The coefficients b_i used in Eq. (2) for mesoscale (denoted by superscript "m") and small-scale (or turbulent) (denoted by superscript "t") sensible heat, moisture, and momentum fluxes scaled by their corresponding total (or turbulent) surface values

Dimensionless fluxes	b_1	b_2	b_3	b_4	b_5	b_6	b_7
Mesoscale flux							
$\langle w'\theta' \rangle$	-3.66	-245.30	-2854.60	0.886	0.971×10^{-1}	-100.50	859.40
$\langle w'q' \rangle$	-6.52	-434.20	6674.10	-221.20	-2620.00	2.49	0.188
$\langle w'u' \rangle$	-1.20	53.50	-118.60	-266.00	3641.50	-0.584	-0.545×10^{-1}
Turbulent flux							
$\langle w'\theta' \rangle$	-2.93	-272.30	-2731.50	-98.30	733.10	-0.364	-0.260×10^{-1}
$\langle w'q' \rangle$	1.08	48.80	-67.30	-1088.30	39 871.10	-130.40	752.20
$\langle w'u' \rangle$	-4.58	-884.40	-8316.90	-386.40	3785.20	0.974	0.526×10^{-1}

Table 4

The coefficients c_i used in Eqs (2) and (3) for mesoscale (denoted by superscript ‘‘ \prime ’’) and small-scale (or turbulent) (denoted by superscript ‘‘ $\prime\prime$ ’’) sensible heat, moisture, and momentum fluxes scaled by their corresponding total (or turbulent) surface values

Dimensionless fluxes	c_1	c_2	c_3	c_4
Mesoscale flux				
$\langle w'\theta'\rangle$	0.00	1.30	-2.45	1.08
$\langle w'q'\rangle$	0.00	-0.101	4.50	-2.88
$\langle w'u'\rangle$	0.140×10^{-2}	-0.825×10^{-1}	0.562	-0.328
Turbulent flux				
$\langle w''\theta''\rangle$	1.00	-2.74	2.64	-0.905
$\langle w''q''\rangle$	1.00	2.73	-5.20	1.87
$\langle w''u''\rangle$	1.00	-3.84	5.12	-2.28

three of the eight parameters ($R_b, z/L_r, \lambda_1, \lambda_2, \lambda_3, \lambda_4, \lambda_5, \lambda_6$) and

$$f_1\left(\frac{z}{z_i}\right) = c_1 + c_2\left(\frac{z}{z_i}\right) + c_3\left(\frac{z}{z_i}\right)^2 + c_4\left(\frac{z}{z_i}\right)^3 \tag{4}$$

The values of coefficients a_i, b_i, c_i , and parameters p_i for mesoscale and turbulent fluxes are given in Tables 1-4.

For the total sensible heat flux scaled by its surface value, the formula is

$$\frac{F - f_1\left(\frac{z}{z_i}\right)}{f_1\left(\frac{z}{z_i}\right)} = (a_1 + a_2\lambda_2 + a_3\lambda_3 + a_4\lambda_4 + a_5\lambda_6 + a_6R_b) + (b_1 + b_2\lambda_2 + b_3\lambda_3 + b_4\lambda_4 + b_5\lambda_6 + b_6R_b)\frac{z}{z_i} \tag{5}$$

where

$$f_1\left(\frac{z}{z_i}\right) = c_1 + c_2\left(\frac{z}{z_i}\right) + c_3\left(\frac{z}{z_i}\right)^2 \tag{6}$$

The values of coefficients a_i, b_i , and c_i are given in Table 5.

Table 5

The coefficients a_i, b_i , and c_i used in Eqs. (4) and (5) for total sensible heat flux scaled by its surface value

Coefficients	a_1	a_2	a_3	a_4	a_5	a_6
$\langle w'\theta'\rangle + \langle w''\theta''\rangle$	-0.546×10^{-1}	-10.20	92.10	3.98	0.410×10^{-2}	0.367×10^{-2}
Coefficients	b_1	b_2	b_3	b_4	b_5	b_6
$\langle w'\theta'\rangle + \langle w''\theta''\rangle$	3.22	289.00	-2593.90	-88.50	-0.387	0.211
Coefficients	c_1	c_2	c_3			
$\langle w'\theta'\rangle + \langle w''\theta''\rangle$	1.0	-1.5	0.37			

Table 6
The coefficients a_i , b_i , and c_i used in Eqs (4) and (5) for total moisture flux scaled by its surface value

Coefficients $(w'q') + (w''q'')$	a_1	a_2	a_3	a_4	a_5	a_6	a_7	a_8	a_9
		0.939×10^{-1}	2.81	8.26	134.70	-0.606×10^{-2}	0.586×10^{-4}	-9.72	91.90
Coefficients $(w'q') + (w''q'')$	b_1		b_3	b_4	b_5	b_6	b_7	b_8	b_9
		2.01	-29.10	65.60	400.70	-0.485	0.308×10^{-1}	-67.90	393.20
Coefficients $(w'q') + (w''q'')$	c_1		c_3						
		1.00	1.80						

Table 7

The values of the coefficients a_i , b_i , c_i , and d_i used in Eqs. (7) and (8) for total momentum flux scaled by its surface value

Coefficients	a_1	a_2	a_3	a_4
$\langle w'u' \rangle + \langle w''u'' \rangle$	-0.240	-8.19	0.264×10^{-1}	-2.49
Coefficients	b_1	b_2	b_3	b_4
$\langle w'u' \rangle + \langle w''u'' \rangle$	-1.61	-91.40	0.22	-34.80
Coefficients	c_1	c_2	c_3	c_4
$\langle w'u' \rangle + \langle w''u'' \rangle$	2.29	117.90	-0.334	49.90
Coefficients	d_1	d_2	d_3	d_4
$\langle w'u' \rangle + \langle w''u'' \rangle$	1.00	-3.97	6.00	-2.87

For the total moisture flux scaled by its surface value, the formula is

$$\frac{F - f_1\left(\frac{z}{z_i}\right)}{f_1\left(\frac{z}{z_i}\right)} = \left[a_1 + a_2\lambda_1 + a_3\lambda_1^2 + a_4\lambda_4 + a_5\lambda_4^2 + a_6\lambda_6 + a_7\lambda_6^2 + a_8\left(\frac{z_i}{L_x}\right)^2 + a_9\left(\frac{z_i}{L_x}\right)^2 \right] + \left[b_1 + b_2\lambda_1 + b_3\lambda_1^2 + b_4\lambda_4 + b_5\lambda_4^2 + b_6\lambda_6 + b_7\lambda_6^2 + b_8\left(\frac{z_i}{L_x}\right) + b_9\left(\frac{z_i}{L_x}\right)^2 \right] \frac{z}{z_i} \quad (7)$$

where $f_1(z/z_i)$ is a quadratic polynomial as expressed in Eq. (6). The values of the coefficients a_i , b_i , and c_i in Eqs. (6) and (7) are given in Table 6.

Table 8

The ratio of mesoscale to turbulent fluxes of heat, moisture, and momentum as a function of dimensionless height, z/z_i , for the FIFE study area. The parameter $L_x = 10$ km and other parameters are given in the text

z/z_i	$\langle w'\theta' \rangle / \langle w''\theta'' \rangle$	$\langle w'u' \rangle / \langle w''u'' \rangle$	$\langle w'q' \rangle / \langle w''q'' \rangle$
0.1	0.21	0.015	0.0085
0.2	0.50	-0.040	0.031
0.3	0.89	-0.16	0.063
0.4	1.37	-0.37	0.11
0.5	1.93	-0.68	0.16
0.6	2.48	-0.91	0.23
0.7	2.71	-0.70	0.32
0.8	1.69	-0.19	0.45
0.9	-5.22	0.50	0.65
1.0	35.5	∞	1.02

Table 9

Same as Table 8 except $L_x = 20$ km

z/z_i	$\langle w'\theta' \rangle / \langle w''\theta'' \rangle$	$\langle w'u' \rangle / \langle w''u'' \rangle$	$\langle w'q' \rangle / \langle w''q'' \rangle$
0.1	0.33	-0.0056	0.0085
0.2	0.77	0.024	0.037
0.3	1.34	0.15	0.087
0.4	2.06	0.49	0.16
0.5	2.92	1.33	0.27
0.6	3.81	2.79	0.42
0.7	4.27	4.07	0.64
0.8	2.76	4.77	0.97
0.9	-8.93	6.61	1.51
1.0	64.5	∞	2.52

For the total momentum flux scaled by its surface value F , the formula is

$$F - f_1 \left(\frac{z}{z_i} \right) = \left[a_1 + a_2 \lambda_4 + a_3 \lambda_6 + a_4 \left(\frac{z_i}{L_x} \right) \right] + \left[b_1 + b_2 \lambda_4 + b_3 \lambda_6 + b_4 \left(\frac{z_i}{L_x} \right) \right] \frac{z}{z_i} + \left[c_1 + c_2 \lambda_4 + c_3 \lambda_6 + c_4 \left(\frac{z_i}{L_x} \right) \right] \left(\frac{z}{z_i} \right)^2 \quad (8)$$

where

$$f_1 \left(\frac{z}{z_i} \right) = d_1 + d_2 \left(\frac{z}{z_i} \right) + d_3 \left(\frac{z}{z_i} \right)^2 + d_4 \left(\frac{z}{z_i} \right)^3 \quad (9)$$

The coefficients a_i , b_i , c_i , and d_i are given in Table 7.

To demonstrate an application of the parameterization scheme, we use Eqs. (3) and (4) to assess the relative importance of mesoscale and turbulent fluxes for the FIFE study area in Kansas. FIFE field program results and an overview of the program are presented in Sellers and coworkers (Sellers et al., 1992a). Using results presented by Smith and coworkers (Smith et al., 1994) and Betts and coworkers (Betts et al., 1992), the parameters required for use in Eqs. (3) and (4) were estimated as: $L = 10-20$ km, $w_* = 1.6$ m s⁻¹, $\delta\theta = 3^\circ\text{C}$, $\Delta\theta = 5^\circ\text{C}$, $z_i = 1$ km, and $U = 4$ m s⁻¹. Values of these parameters, of course, vary from day to day but these estimates will provide insight as to the relative importance of mesoscale fluxes in that study area.

Using $L = 10$ km and 20 km, the ratio of mesoscale to turbulent fluxes of heat, moisture, and momentum as a function of height is presented in Tables 8 and 9. It is seen that near the surface the turbulent fluxes are dominant; however, in the upper portion of the boundary layer the mesoscale fluxes (especially those of sensible heat and momentum) are dominant. This conclusion is consistent with the interpretation of Smith and coworkers (Smith et al., 1994) and others who participated in the FIFE study, in that mesoscale fluxes did occur. This is also consistent with the estimate of FIFE-area surface fluxes obtained

from FIFE-area averaged variables which are essentially identical to the linear averages of individual point-specific fluxes, as reported by Sellers and coworkers (Sellers et al., 1992b), because the total fluxes are always dominated by turbulence, and the mesoscale ascent is small near the surface.

4. Conclusions

A procedure to represent mesoscale and subgrid-scale fluxes in a cloud-free environment over flat heterogeneous landscapes is introduced. New non-dimensional parameters were presented with which a parameterization of this effect for use in larger scale models was constructed. While additional parameters, such as the Coriolis term f need to be considered, and wind speeds less than 3 m s^{-1} need to be included, the framework presented in this paper has an apparent universal form which should be used for further study, and validation against observations. Also, the generality of the empirical coefficients used to construct the parameterizations needs to be assessed.

One of the conclusions is that one can ignore mesoscale fluxes when they are a small fraction of the turbulence fluxes. For these situations, the one-dimensional parameterizations introduced a number of other authors (Avissar and Pielke, 1989; Sellers et al., 1992b; Miller, 1993) could be used.

Acknowledgements

This work was supported by the National Science Foundation under grant no. ATM-8915265 and ATM-9306754, the National Aeronautics and Space Administration under grant no. NAG 5-2078, S-01, and the Climate System Modeling Program through sub-contract no. UCAR S9361. The review of this paper by Roni Avissar was very much appreciated. The paper was ably edited by Dallas McDonald.

References

- André, J.C., Bougeault, P., Mahfouf, J.F., Mascart, P., Noilhan, J. and Pinty, J.P., 1989a. Impact of forests on mesoscale meteorology. *Phil. Trans. R. Soc. London*, 324: 407–422.
- André, J.C., Goutorbe, J.P., Schmugge, T. and Perrier, A., 1989b. HAPEX-MOBILHY: Results from a large-scale field experiment. In: A. Rango (Editor), *Remote Sensing and Large-scale Global Processes*. International Association of Hydrological Sciences, Wallingford, UK, pp. 13–20.
- Arritt, R.W. and Clark, C.A., 1994. Functional relationships among soil moisture, vegetation cover, and surface fluxes. In: *Proc. Special Session on Hydrometeorology*, AMS, MA, 1994 March 7–10, San Diego, CA.
- Avissar, R. and Chen, F., 1993. Development and analysis of prognostic equations for mesoscale kinetic energy and mesoscale (subgrid-scale) fluxes for large-scale atmospheric models. *J. Atmos. Sci.*, 50: 3751–3774.
- Avissar, R. and Pielke, R.A., 1989. A parameterization of heterogeneous land surfaces for atmospheric numerical models and its impact on regional meteorology. *Mon. Weather Rev.*, 117: 2113–2136.
- Avissar, R. and Verstraete, M.M., 1990. The representation of continental surface processes in atmospheric models. *Rev. Geophys.*, 28: 35–52.

- Balling, Jr., R.C., 1988. The climatic impact of a Sonoran vegetation discontinuity. *Climatic Change*, 13: 99–109.
- Beljaars, A.C.M. and Holtlag, A.A.M., 1991. Flux parameterization over land surfaces for atmospheric models. *J. Appl. Meteorol.*, 30: 327–341.
- Betts, A.K. and Beljaars, A.C.M., 1993. Estimation of effective roughness length for heat and momentum from FIFE data. *Atmos. Res.*, 30: 251–261.
- Betts, A.K., Desjardins, R.L. and MacPherson, J.I., 1992. Budget analysis of the boundary layer grid flights during FIFE 1987. *J. Geophys. Res.*, 97: 18 533–18 546.
- Bolle, H.J., André, J.C., Arrue, J.L., Barth, H.K., Bessemoulin, P. et al., 1993. EFEDA: European Field Experiment in a Desertification threatened Area. *Ann. Geophys.*, 11: 173–189.
- Bonan, G.B., Pollard, D. and Thompson, S.L., 1993. Influence of subgrid-scale heterogeneity in leaf area index, stomatal resistance, and soil moisture on grid-scale land-atmosphere interactions. *J. Climate*, 6: 1882–1897.
- Claussen, M., 1991. Estimation of areally-averaged surface fluxes. *Boundary-Layer Meteorol.*, 54: 387–410.
- Cooter, E.J., Eder, B.K., LeDuc, S.K. and Trippi, L., 1993. General circulation model output for forest climate change research and applications. Southeast. Exp. Stn. Tech. Bull., Asheville, NC, 38 pp.
- Cotton, W.R. and Pielke, R.A., 1995. *Human Impacts on Weather and Climate*, Cambridge University Press, New York.
- Dalu, G.A. and Pielke, R.A., 1993. Vertical heat fluxes generated by mesoscale atmospheric flow induced by thermal inhomogeneities in the PBL. *J. Atmos. Sci.*, 50: 919–926.
- Dalu, G.A., Pielke, R.A., Avissar, R., Kallos, G., Baldi, M. and Guerrini, A., 1991a. Linear impact of thermal inhomogeneities on mesoscale atmospheric flow with zero synoptic wind. *Ann. Geophys.*, 9: 641–647.
- Dalu, G.A., Baldi, M., Pielke, R.A., Lee, T.J. and Colacino, M., 1991b. Mesoscale vertical velocities generated by stress changes in the boundary layer: linear theory. *Ann. Geophys.*, 9: 648–653.
- Doran, J.C., Barnes, F.J., Coulter, R.L., Crawford, T.L., Baldocchi, D.D. et al., 1992. The Boardman regional flux experiment. *Bull. Am. Meteorol. Soc.*, 73: 1785–1795.
- Garratt, J.R., 1992. *The atmospheric boundary layer*. Cambridge Atmospheric and Space Science Series, Cambridge University, New York.
- Gash, J.H.C. and Shuttleworth, W.J., 1991. Tropical deforestation: Albedo and the surface-energy balance. *Climatic Change*, 19: 123–133.
- Gash, J.H.C., Wallace, J.S., Lloyd, C.R., Dolman, A.J., Sivakumar, M.V.K. and Renard, C., 1991. Measurements of evaporation from fallow Sahelian Savannah at the start of the dry season. *Q. J. R. Meteorol. Soc.*, 117: 749–760.
- Guo, Y. and Schuepp, P.H., 1994. An analysis of the effect of local heat advection on evaporation over wet and dry surface strips. *J. Climate*, 7: 641–652.
- Hadfield, M.G., Cotton, W.R. and Pielke, R.A., 1991. Large-eddy simulations of thermally-forced circulations in the convective boundary layer. Part I: A small-scale circulation with zero wind. *Boundary-Layer Meteorol.*, 57: 79–114.
- Hadfield, M.G., Cotton, W.R. and Pielke, R.A., 1992. Large-eddy simulations of thermally forced circulations in the convective boundary layer. Part II: The effect of changes in wavelength and wind speed. *Boundary-Layer Meteorol.*, 58: 307–328.
- Henderson-Sellers, A., Yang, Z.-L. and Dickinson, R.E., 1993. The project for intercomparison of land-surface parameterization schemes. *Bull. Am. Meteorol. Soc.*, 74: 1335–1349.
- Kosta, R.D. and Suarez, M.J., 1992. A comparative analysis of two land surface heterogeneity representations. *J. Climate*, 5: 1379–1390.
- Li, B. and Avvisar, R., 1994. The impact of spatial variability of land-surface heat fluxes. *J. Climate*, 7: 527–537.
- Lynn, B.H., Abramopoulos, F. and Avissar, R., 1995. Using similarity theory to parameterize mesoscale heat fluxes generated by subgrid-scale landscape discontinuities in GCMs. *J. Climate*, 8: 932–951.
- Mahrt, L., 1987. Grid-averaged surface fluxes. *Mon. Weather Rev.*, 115: 1550–1560.
- Mahrt, L. and Ek, M., 1993. Spatial variability of turbulent fluxes and roughness lengths in HAPEX-MOBILHY. *Boundary-Layer Meteorol.*, 65: 381–400.
- Mahrt, L., Sun, J., Vickers, D., Macpherson, J.I. and Pederson, J.R., 1994a. Observations of fluxes and inland breezes over a heterogeneous surface. *Boundary-Layer Meteorol.*, *J. Atmos. Sci.*, 51, 2484.
- Mahrt, L., MacPherson, J.I. and Desjardins, R., 1994b. Observations of fluxes over heterogeneous surfaces. *Boundary-Layer Meteorol.*, 67: 345–367.

- Manqian, M. and Jinjun, J., 1993. A coupled model on land–atmosphere interactions simulating the characteristics of the PBL over a heterogeneous surface. *Boundary-Layer Meteorol.*, 66: 247–264.
- Mason, P.J., 1988. The formation of areally averaged roughness lengths. *Q. J. R. Meteorol. Soc.*, 114: 399–420.
- Miller, N., 1993. Applications of a hierarchical systems flux scheme for interactively coupling subgrid land surface models with atmospheric models. University of California–Lawrence Livermore National Laboratory Technical Report, UCRL-JC-114100, 27 pp.
- Noilhan, J., André, J.C., Bougeault, P., Goutorbe, J. and Lacarrere, P., 1991. Some aspects of the HAPEX-MOBILHY programme: The data base and the modelling strategy. *Surv. Geophys.*, 12: 31–61.
- Pielke, R.A., 1984. *Mesoscale Meteorological Modeling*. Academic, New York, NY.
- Pielke, R.A., Dalu, G., Snook, J.S., Lee, T.J. and Kittel, T.G.F., 1991. Nonlinear influence of mesoscale land use on weather and climate. *J. Climate*, 4: 1053–1069.
- Pielke, R.A., Cotton, W.R., Walko, R.L., Tremback, C.J., Lyons, W.A., Grasso, L.D., Nicholls, M.E., Moran, M.D., Wesley, D.A., Lee, T.J. and Copeland, J.H., 1992. A comprehensive meteorological modeling system—RAMS. *Meteorol. Atmos. Phys.*, 49: 69–91.
- Pielke, R.A., Rodriguez, J.H., Eastman, J.L., Walko, R.L. and Stocker, R.A., 1993a. Influence of albedo variability in complex terrain on mesoscale systems. *J. Climate*, 6: 1798–1806.
- Pielke, R.A., Dalu, G., Lee, T.J., Rodriguez, H., Eastman, J. and Kittel, T.G.F., 1993b. Mesoscale parameterization of heat fluxes due to landscape variability for use in general circulation models. In: H.J. Bolle, R.A. Feddes, P. Kalma (Editors), *Exchange Processes at the Land Surface of Space of Time Scales*. International Association of Hydrological Sciences, Publication # 212, IAHS Press, Wallingford, UK, 331.
- Raupach, M.R., 1991. Vegetation–atmosphere interaction in homogeneous and heterogeneous terrain: Some implications of mixed layer dynamics. In: A. Henderson-Sellers and A.J. Pitman (Editors), *Vegetation and Climate Interactions in Semi-arid Regions*. Kluwer Academic, Dordrecht, pp. 105–120.
- Schädler, G., Kalthoff, N. and Fiedler, F., 1990. Validation of a model for heat, mass, and momentum exchange over vegetated surfaces using LOTREX 10E/HIBE88 data. *Contrib. Atmos. Phys.*, 63: 85–100.
- Segal, M. and Arritt, R.W., 1992. Non-classical mesoscale circulations caused by surface sensible heat-flux gradients. *Bull. Am. Meteorol. Soc.*, 73: 1593–1604.
- Segal, M., Avissar, R., McCumber, M.C. and Pielke, R.A., 1988. Evaluation of vegetation effects on the generation and modification of mesoscale circulations. *J. Atmos. Sci.*, 45: 2268–2292.
- Segal, M., Schreiber, W., Kallos, G., Pielke, R.A., Garratt, J.R., Weaver, J., Rodi, A. and Wilson, J., 1989. The impact of crop areas in northeast Colorado on midsummer mesoscale thermal circulations. *Mon. Weather Rev.*, 117: 809–825.
- Sellers, P.J., Hall, F.G., Asrar, G., Strelbel, D.E. and Murphy, R.E., 1992a. An overview of the First International Satellite Land Surface Climatology Project (ISLSCP) Field Experiment (FIFE). *J. Geophys. Res.*, 97: 18 345–18 371.
- Sellers, P.J., Hall, F.G., Margolis, H., Kelly, B., Baldocchi, D., den Hartog, J., Cilhar, J., Ryan, M. Goodison, B., Crill, P., Ranson, D., Lettenheimer and Wickland, D., 1995. The Boreal Ecosystems Atmosphere Study (BOREAS): an overview and early results from the 1994 field year. *Bull. Amer. Meteor. Soc.*, 76: 1549–1577.
- Sellers, P.J., Heiser, M.D. and Hall, F.G., 1992b. Relations between surface conductance and spectral vegetation indices at intermediate (10 m² to 15 km²) length scales. *J. Geophys. Res.*, 97: 19 033–19 059.
- Shuttleworth, W.J., 1985. Daily variations of temperature and humidity within and above Amazonian forest. *Weather*, 40: 102–108.
- Smith, E.A., Hsu, A.Y., Crosson, W.L., Field, R.T., Fritschen, L.J. et al., 1992. Area-averaged surface fluxes and their time–space variability over the FIFE experimental domain. Paper No. 91JD03060, *J. Geophys. Res.*, 97: 18 599–18 622.
- Smith, E.A., Wai, M.M.-K., Cooper, H.J., Rubes, M.T. and Hsu, A., 1994. Linking boundary layer circulations and surface processes during FIFE 89. Part 1: Observational analysis. *J. Atmos. Sci.*, 51: 1497.
- Wallace, J.S., Wright, I.R. and Stewart, J.B., 1991. The Sahelian Energy Balance Experiment (SEBEX): Ground based measurements and their potential for spatial extrapolation using satellite data. *Adv. Space Res.*, 11: 131–142.
- Wierenga, J., 1986. Roughness-dependent geographical interpolation of surface wind speed averages. *Q. J. R. Meteorol. Soc.*, 112: 867–889.

- Wright, I.R., Gash, J.H.C., da Rocha, H.R., Shuttleworth, W.J., Nobre, C.A., Maitelli, G.T., Zamparoni, C.A.G.P. and Carvalho, P.R.A., 1992. Dry season micrometeorology of central Amazonian ranch-land. *Q. J. R. Meteorol. Soc.*, 118: 1083–1099.
- Wood, E.F., Lettenmaier, D.P. and Zartarian, V.G., 1992. A land-surface hydrology parameterization with subgrid variability for general circulation models. *J. Geophys. Res.*, 97: 2717–2728.
- Xian, Z. and Pielke, R.A., 1991. The effects of width of land masses on the development of sea breezes. *J. Appl. Meteorol.*, 30: 1280–1304.
- Zeng, X., 1992. Chaos theory and its application in the atmosphere. Atmospheric Science Paper No. 504, Colorado State University, Dept. of Atmosphere Science, Fort Collins, CO.
- Zeng, X. and Pielke, R.A., 1993a. Error-growth dynamics and predictability of surface thermally-induced atmospheric flow. *J. Atmos. Sci.*, 50: 2817–2844.
- Zeng, X. and Pielke, R.A., 1993b. Predictability and chaos in atmospheric coherent structures. In: IAMAP-IAHS '93 Joint International Meeting, The Sixth Scientific Assembly of the International Association of Meteorology and Atmospheric Physics, Yokohama, Japan, 1993 July 11–23.
- Zeng, X. and Pielke, R.A., 1995a. Further study on the predictability of landscape-induced atmospheric flow. *J. Atmos. Sci.*, 52: 1680–1698.
- Zeng, X. and Pielke, R.A., 1995b. Landscape-induced atmospheric flow and its parameterization in large-scale numerical models. *J. Climate*, 8: 1156–1177.